JACC: CARDIOVASCULAR IMAGING VOL. 10, NO. 7, 2017

ISSN 1936-878X/$36.00
http://dx.doi.org/10.1016/j.jcmg.2016.09.028

Integrating CT Myocardial Perfusion and CT-FFR in the Work-Up of Coronary Artery Disease

Adriaan Coenen, MD,[a,b] Alexia Rossi, MD, PhD,[a,c] Marisa M. Lubbers, MD,[a,b] Akira Kurata, MD, PhD,[b] Atsushi K. Kono, MD, PhD,[b] Raluca G. Chelu, MD,[b] Sabrina Segreto, MD,[c] Marcel L. Dijkshoorn, RT,[b] Andrew Wragg, PhD,[c] Robert-Jan M. van Geuns, MD, PhD,[a,b] Francesca Pugliese, MD, PhD,[c] Koen Nieman, MD, PhD[a,b]

JACC: CARDIOVASCULAR IMAGING CME/MOC

CME/MOC Editor: Ragavendra R. Baliga, MD

This article has been selected as this issue's CME/MOC activity, available online at http://www.acc.org/jacc-journals-cme by selecting the *JACC* Journals CME/MOC tab.

Accreditation and Designation Statement

The American College of Cardiology Foundation (ACCF) is accredited by the Accreditation Council for Continuing Medical Education (ACCME) to provide continuing medical education for physicians.

The ACCF designates this Journal-based CME/MOC activity for a maximum of 1 *AMA PRA Category 1 Credit(s)* ™. Physicians should only claim credit commensurate with the extent of their participation in the activity.

Method of Participation and Receipt of CME/MOC Certificate

To obtain credit for this CME/MOC activity, you must:

1. Be an ACC member or *JACC: Cardiovascular Imaging* subscriber.
2. Carefully read the CME/MOC-designated article available online and in this issue of the journal.
3. Answer the post-test questions. At least 2 out of the 3 questions provided must be answered correctly to obtain CME/MOC credit.
4. Complete a brief evaluation.
5. Claim your CME/MOC credit and receive your certificate electronically by following the instructions given at the conclusion of the activity.

CME/MOC Objective for This Article: After reading this article the reader should be able to: 1) understand the diagnostic performance of a coronary CT angiography and how to interpret the results in the context of a functional reference test such as invasive FFR; 2) understand the principles of CT derived FFR; and 3) understand the background of a dynamic CT myocardial perfusion scan.

CME/MOC Editor Disclosure: *JACC: Cardiovascular Imaging* CME/MOC Editor Ragavendra R. Baliga, MD, has reported that he has no relationships to disclose.

Author Disclosures: Drs. Coenen, Lubbers, and Nieman were supported by a grant from the Dutch Heart Foundation (NHS 2014T061). This work forms part of the translational research portfolio of the National Institute for Health Research Cardiovascular Biomedical Research Unit at Barts, which is supported and funded by the National Institute for Health Research (Dr. Pugliese). Dr. Rossi is a recipient of a Training Grant from the European Society of Cardiology (2014). Dr. Dijkshoorn is a consultant for Siemens AG. Dr. van Geuns has received speaking fees from Abbott Vascular. Dr. Nieman has received institutional research support from Bayer Healthcare, GE Healthcare, Siemens Medical Solutions, and HeartFlow. Dr. Pugliese has received research support from Siemens Healthcare; and speaking fees from Bracco Diagnostics. All other authors have reported that they have no relationships relevant to the contents of this paper to disclose.

Medium of Participation: Print (article only); online (article and quiz).

CME/MOC Term of Approval

Issue Date: July 2017
Expiration Date: June 30, 2018

From the [a]Department of Cardiology, Erasmus University Medical Center, Rotterdam, the Netherlands; [b]Department of Radiology, Erasmus University Medical Center, Rotterdam, the Netherlands; and the [c]Centre for Advanced Cardiovascular Imaging, NIHR Cardiovascular Biomedical Research Unit at Barts, William Harvey Research Institute, Barts and The London School of Medicine and Dentistry, Queen Mary University of London & St. Bartholomew's Hospital, London, United Kingdom. Drs. Coenen, Lubbers, and Nieman were supported by a grant from the Dutch Heart Foundation (NHS 2014T061). This work forms part of the translational research portfolio of the National Institute for Health Research Cardiovascular Biomedical Research Unit at Barts, which is supported and funded by the National Institute for Health Research (Dr. Pugliese). Dr. Rossi is a recipient of a Training Grant from the European Society of Cardiology (2014). Dr. Dijkshoorn is a consultant for Siemens AG. Dr. van Geuns has received speaking fees from Abbott Vascular. Dr. Nieman has received institutional research support from Bayer Healthcare, GE Healthcare, Siemens Medical Solutions, and HeartFlow. Dr. Pugliese has received research support from Siemens Healthcare; and speaking fees from Bracco Diagnostics. All other authors have reported that they have no relationships relevant to the contents of this paper to disclose. Drs. Pugliese and Nieman contributed equally to this work.

Manuscript received August 2, 2016; accepted September 1, 2016.

Integrating CT Myocardial Perfusion and CT-FFR in the Work-Up of Coronary Artery Disease

Adriaan Coenen, MD,[a,b] Alexia Rossi, MD, PhD,[a,c] Marisa M. Lubbers, MD,[a,b] Akira Kurata, MD, PhD,[b] Atsushi K. Kono, MD, PhD,[b] Raluca G. Chelu, MD,[b] Sabrina Segreto, MD,[c] Marcel L. Dijkshoorn, RT,[b] Andrew Wragg, PhD,[c] Robert-Jan M. van Geuns, MD, PhD,[a,b] Francesca Pugliese, MD, PhD,[c] Koen Nieman, MD, PhD[a,b]

ABSTRACT

OBJECTIVES The aim of this study was to investigate the individual and combined accuracy of dynamic computed tomography (CT) myocardial perfusion imaging (MPI) and computed tomography angiography (CTA) fractional flow reserve (FFR) for the identification of functionally relevant coronary artery disease (CAD).

BACKGROUND Coronary CTA has become an established diagnostic test for ruling out CAD, but it does not allow interpretation of the hemodynamic severity of stenotic lesions. Two recently introduced functional CT techniques are dynamic MPI and CTA FFR using computational fluid dynamics.

METHODS From 2 institutions, 74 patients (n = 62 men, mean age 61 years) planned for invasive angiography with invasive FFR measurement in 142 vessels underwent CTA imaging and dynamic CT MPI during adenosine vasodilation. A patient-specific myocardial blood flow index was calculated, normalized to remote myocardial global left ventricular blood flow. CTA FFR was computed using an on-site, clinician-operated application. Using binary regression, a single functional CT variable was created combining both CT MPI and CTA FFR. Finally, stepwise diagnostic work-up of CTA FFR with selective use of CT MPI was simulated. The diagnostic performance of CT MPI, CTA FFR, and CT MPI integrated with CTA FFR was evaluated using C statistics with invasive FFR, with a threshold of 0.80 as a reference.

RESULTS Sensitivity, specificity, and accuracy were 73% (95% confidence interval [CI]: 61% to 86%), 68% (95% CI: 56% to 80%), and 70% (95% CI: 62% to 79%) for CT MPI and 82% (95% CI: 72% to 92%), 60% (95% CI: 48% to 72%), and 70% (63% to 80%) for CTA FFR. For CT MPI integrated with CTA FFR, diagnostic accuracy was 79% (95% CI: 71% to 87%), with improvement of the area under the curve from 0.78 to 0.85 ($p < 0.05$). Accuracy of the stepwise approach was 77%.

CONCLUSIONS CT MPI and CTA FFR both identify functionally significant CAD, with comparable accuracy. Diagnostic performance can be improved by combining the techniques. A stepwise approach, reserving CT MPI for intermediate CTA FFR results, also improves diagnostic performance while omitting nearly one-half of the population from CT MPI examinations. (J Am Coll Cardiol Img 2017;10:760–70)

Computed tomography angiography (CTA) has become an established diagnostic technique to assess coronary artery disease (CAD). However, CTA provides only anatomic information and tends to overestimate stenosis severity, particularly in the presence of calcifications (1,2). Over the past decade, functional parameters have become more important for management decisions, in particular with regard to mechanical revascularization. Catheter-based fractional flow reserve (FFR) is currently regarded as the reference for the assessment of the hemodynamic severity of CAD (3–5). The relation between angiographic stenosis and functional significance is diffuse. Compared with invasive FFR, the specificity of CTA imaging with a conventional 50% stenosis threshold is low (6–8).

Several strategies have been developed for the functional assessment of CAD by cardiac computed tomography (CT). In this study, we investigated the diagnostic performance CTA and 2 recently introduced functional cardiac CT techniques, dynamic CT myocardial perfusion imaging (MPI) and CTA computational FFR, using an application that can be performed locally on site.

ABBREVIATIONS AND ACRONYMS

AIF = arterial input function

AUC = area under the curve

CAD = coronary artery disease

CT = computed tomography

CTA = computed tomography angiography

FFR = fractional flow reserve

IQR = interquartile range

MBF = myocardial blood flow

$MBF(LV)_{75\%}$ = myocardial blood flow of the myocardial segment representing the 75th percentile

MPI = myocardial perfusion imaging

METHODS

STUDY DESIGN. At 2 centers 76 patients with known or suspected CAD underwent CTA and CT MPI <14 days before clinically indicated invasive coronary angiography (9). By study protocol, FFR measurements were performed in vessels with visual diameter stenoses between 30% and 90%.

Exclusion criteria were age <40 years, invasive FFR measurement not performed, impaired renal function, possible pregnancy or breastfeeding, body weight >120 kg, use of clopidogrel, total occlusion of a dominant coronary artery, nondiagnostic CTA image quality, and contraindications to iodine contrast material or adenosine.

SEE PAGE 771

The study protocol was compliant with the Declaration of Helsinki and received approval from the research ethics committee at each institution. All patients provided written informed consent.

CTA IMAGING. All patients received sublingual nitroglycerin before CTA studies. Beta-blockers were used only very selectively before CTA studies because of potential interaction with the adenosine response needed for dynamic CT MPI. The prospective electrocardiographically triggered axial scan mode was used, with an exposure window during diastole and/or systole depending on the heart rate. Tube current and tube voltage were selected semiautomatically on the basis of body size. A test bolus acquisition was performed using 15 ml of contrast medium followed by a 40-ml saline chaser. For CTA imaging, a contrast bolus of 50 to 60 ml (depending on iodine concentration) was injected to achieve an iodine delivery rate of 2.2 g/s, followed by a 40-ml saline bolus chaser. Images were reconstructed with a medium smooth kernel (B26, Bv40), slice thickness of 0.5 mm, and an increment of 0.3 mm.

The CT angiograms were evaluated by an experienced reader, blinded to all other modalities. On a per vessel basis, stenoses were classified as recommended by the Society of Cardiovascular Computed Tomography: normal, 0% luminal diameter reduction; minimal, 1% to 24% reduction; mild, 25% to 49% reduction; moderate, 50% to 69% reduction; severe, 70% to 99% reduction; and occluded, 100% reduction (10). A stenosis grade of 50% or greater on CTA was considered to indicate angiographically significant stenosis. The most severe stenosis on coronary CTA proximal to the FFR pressure wire position was defined as the lesion of interest.

DYNAMIC CT MPI. All patients were instructed to refrain from caffeine intake 24 h prior to the examination. In both antecubital veins, 18-gauge cannulas were placed. Blood pressure and electrocardiogram were monitored during the examination. Seventy-one patients were scanned using a second-generation dual-source CT scanner and 3 using a third-generation dual-source system (SOMATOM Definition Flash and SOMATOM Force, Siemens, Forchheim, Germany).

The scan range of dynamic CT MPI was planned using a low-dose noncontrast scan acquired during systole. Adenosine was infused over 3 to 6 min at 140 μg/kg/min. Contrast media (50 or 60 ml) was injected resulting in an iodine delivery rate of 2.2 g/s, followed by a saline bolus of 40 ml. CT MPI examinations were started 5 s after contrast injection was started, using an axial scan mode triggered at 250 ms after the R wave (end-systolic). Imaging of the complete left ventricle required a shuttle-mode acquisition technique. By moving the table back and forth after each acquisition, 2 series of images were collected that together covered the entire myocardium. Depending on heart rate, scans were performed every second or third heart cycle, resulting in a series of 10 to 15 phases acquired over a period of approximately 30 s (11).

The following scan parameters were used: for the second-generation dual-source scanner, collimation of 2 × 64 × 0.6 mm, gantry rotation time of 280 ms, temporal resolution of 75 ms, tube voltage and current of 100 kV and 300 mA or 80 kV and 370 mA per rotation, and shuttle-mode z-axis coverage of 73 mm; for the third-generation dual-source scanner, collimation of 2 × 96 × 0.6 mm, gantry rotation time of 250 ms, temporal resolution of 66 ms, tube voltage and current of 80 kV and 300 mA (Care-kV was used as a reference), and shuttle-mode z-axis coverage of 102 mm.

CT MPI POST-PROCESSING. The CT myocardial perfusion images were reconstructed using a dedicated kernel for reduction of iodine beam-hardening artifacts (b23f, Qr36) and analyzed using a CT MPI software package (Volume Perfusion CT body, Siemens). Motion correction was applied if necessary to correct for breathing-related displacement of the left ventricle. The change of attenuation in the myocardium over time was computed from time-attenuation curves. For quantification of myocardial blood flow (MBF), the influx of contrast medium was measured using the arterial input function (AIF). The AIF was sampled in the descending aorta.

FIGURE 1 Case Example of a 65-Year-Old Man Presenting With Stable Exercise-Related Chest Pain

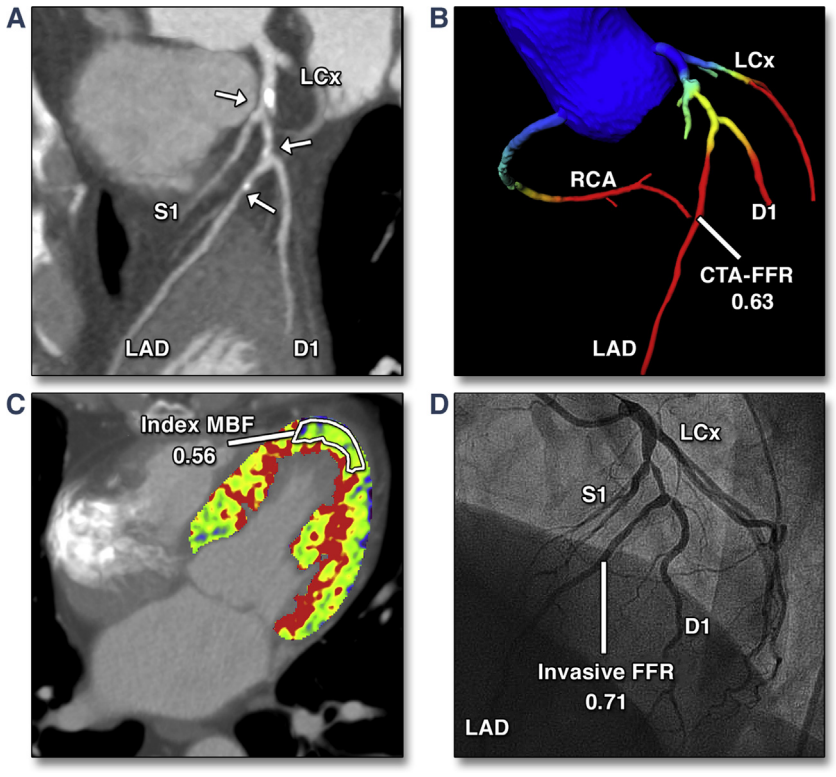

(A) Computed tomography angiography (CTA) demonstrated sequential partly calcified moderate stenoses in the left anterior descending coronary artery (LAD). **(B)** The CTA fractional flow reserve (FFR) simulation demonstrated a significant pressure drop (CTA FFR 0.63). **(C)** Computed tomography (CT) myocardial perfusion image fused with anatomic CT imaging for illustration purposes shows a perfusion defect in the anterior wall, classified as ischemic with a measured index myocardial blood flow (MBF) value of 0.56. **(D)** The corresponding invasive angiography shows the sequential stenosis in the LAD, with an invasively measured FFR of 0.71. Additionally (not shown directly), the left circumflex coronary artery (LCx) also had a hemodynamically relevant stenosis with an invasive FFR of 0.70. The right coronary artery (RCA) was directly stented. D1 = first diagonal branch; S1 = septal branch.

Precision of the AIF was increased by including both the cranial and caudal sections (double sampling). For quantification of the MBF, the myocardial time-attenuation curves were coupled with the AIF using a hybrid deconvolution model. The model uses a simplified impulse residue function for modeling the interaction between intracellular and extracellular compartments. On a per voxel basis, MBF was computed by dividing the convoluted maximal slope of the myocardial time-attenuation curve by the maximum AIF (11–13). MBF maps were reconstructed as a stack of color-coded images with a slice thickness of 3.0 mm and an increment of 1.5 mm.

CT MYOCARDIAL PERFUSION IMAGE ANALYSIS. CT myocardial perfusion images were analyzed with disclosure of which vessels were interrogated by invasive FFR as well as coronary dominance to ensure correct coronary-myocardial interpretation. Readers were blinded to the results of CTA imaging and invasive coronary angiography and all other medical information.

From the MBF map, the slice best representing the myocardium associated with the vessel of interest was selected. Within this cross section, a polygonal region of interest with a minimal area of 50 mm^2 was placed to sample the MBF within the suspected perfusion defect (Syngo Via 2.0, Siemens).

Because CT MPI studies have demonstrated that the global MBF value varies among patients, an index MBF value was applied with normalization for interindividual differences in myocardial flow (12,14,15).

Prototype software (Cardiac Functional Analysis, Siemens) was used to generate a polar map for MBF,

FIGURE 2 Inclusion Flowchart

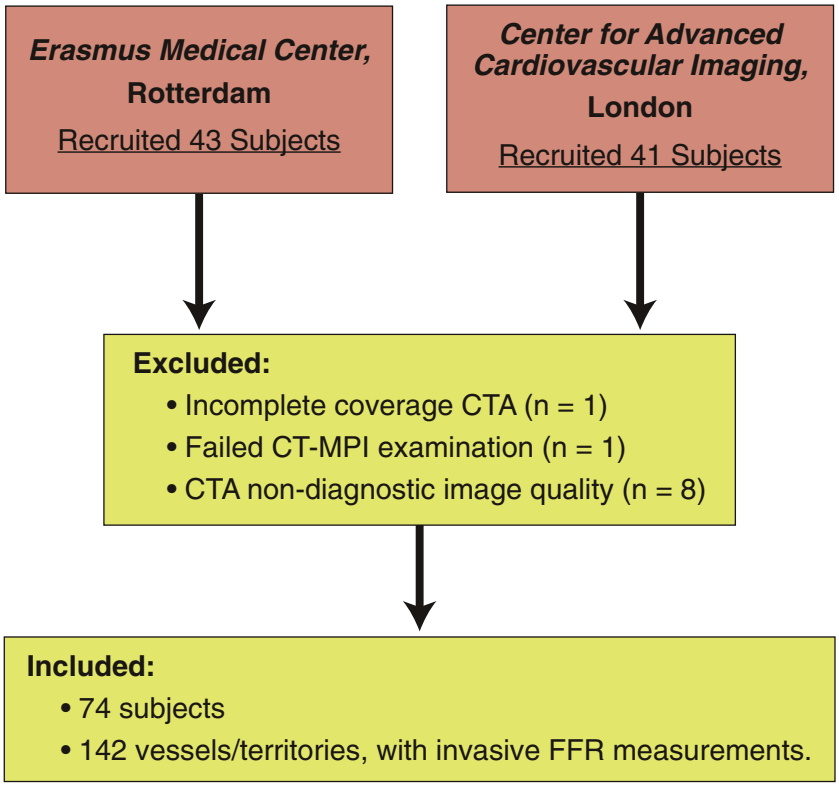

In total, 84 subjects were recruited at 2 sites. Ten patients were excluded, resulting in a total of 74 patients and 142 vessels and territories included in the study. MPI = myocardial perfusion imaging; other abbreviations as in Figure 1.

fitting the modified 17-segment American Heart Association myocardial model onto the CT MPI MBF maps (16). The index MBF value was calculated as the ratio between the MBF sample and the MBF of the myocardial segment representing the 75th percentile, $MBF(LV)_{75\%}$:

$$\text{indexed MBF} = \text{measured MBF}/MBF(LV)_{75\%}$$

CTA FFR. On-site CTA FFR was computed using a dedicated clinician-operated prototype application (cFFR version 1.4, Siemens, not currently commercially available). From a CTA dataset with optimal image quality, a 3-dimensional coronary model was semiautomatically segmented, after which markers were manually placed proximal and distal to each stenotic lesion. The CTA FFR algorithm is composed of a hybrid model using a reduced-order model in the nonstenotic regions and pressure-drop models in the stenotic regions. On the basis of allometric scaling laws, the resting total coronary blood flow is estimated on the basis of the left ventricular mass derived automatically from CTA imaging (17). The resting total coronary blood flow is distributed over the 3-dimensional coronary model. By reducing the microvascular resistance by a factor of 0.21, similar to

TABLE 1 Patient Characteristics (n = 74)

Age, yrs	60.9 ± 9.1
Male	62 (84)
Body mass index, kg/m^2*	26.9 ± 3.6
Cardiovascular risk factors	
Hypertension	40 (54)
Dyslipidemia	45 (61)
Diabetes	15 (20)
Family history of CAD	27 (37)
Smoking within the last year	33 (45)
Prior myocardial infarction†	8 (11)
Prior percutaneous coronary intervention†	4 (5)
Agatston coronary calcium score	289 (74–849)

Values are mean ± SD, n (%), or median (interquartile range). *In 2 patients, height and weight data were not available. †Not in the vessel territories interrogated by invasive fractional flow reserve.
CAD = coronary artery disease.

values achieved by adenosine infusion, a hyperemic state can be simulated (18). By comparing the computed pressures in the aorta and distal to the coronary lesion during simulated hyperemia, an FFR value can be determined. FFR values are computed throughout the coronary arteries and can be superimposed as color gradients onto a 3-dimensional coronary model (19).

After the CTA FFR map was rendered, the sample location of the invasive FFR pressure wire was released. Without making any changes to the CTA FFR model, or revealing the invasive FFR results, the simulated FFR value at the corresponding invasive FFR pressure wire position was recorded (**Figure 1**). A CTA FFR value ≤0.80 was considered as hemodynamically significant.

INVASIVE ANGIOGRAPHY AND FFR. Invasive coronary angiography was performed according to local clinical standards. By study protocol, invasive FFR assessment was performed in all vessels with diameter reduction between 30% and 90%. An FFR pressure wire (PressureWire Aeris/Certus, St. Jude Medical, St. Paul, Minnesota, or Prime/Combo Wire, Volcano, San Diego, California) was positioned distal to the stenosis of interest, after which hyperemia was induced by intravenous infusion of adenosine at 140 μg/kg/min. FFR ≤0.80 was considered hemodynamically significant. To coregister the location of the invasive FFR measurement and CTA FFR, an independent observer without knowledge of the angiographic or functional results identified the invasive FFR sample location on the fluoroscopy images and marked the corresponding location onto the CTA images.

STATISTICAL ANALYSIS. Absolute variables are represented as totals and percentages and continuous variables as mean ± SD or median (interquartile range [IQR]). Effective radiation dose was calculated using a conversion factor of 0.014.

The combined performance of CTA, CT MPI, and CTA FFR was investigated using binary logistic regression (Online Appendix).

Stepwise diagnostic work-up based on CTA FFR with restrictive use of CT MPI was designed by determining the CTA FFR thresholds that resulted in sensitivity of 90% (lower threshold) and specificity of 75% (upper threshold). Vessels with CTA FFR values within this range (the CTA FFR intermediate zone) were reclassified according to the results of CT MPI.

The CT MPI, CTA FFR, and combined CT MPI and CTA FFR values for normal and ischemic territories were compared using an unpaired, 2-sided independent Student *t* test. Correlation between CT MPI and

FIGURE 3 Receiver-Operating Characteristic Curve

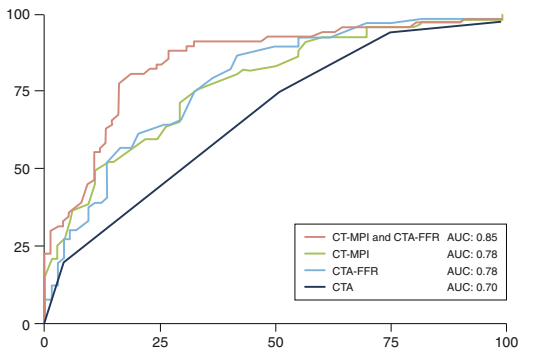

Analysis per vessel or territory, using invasive fractional flow reserve (FFR) as reference. The area under the curve (AUC) for computed tomography (CT) myocardial perfusion imaging (MPI) and FFR (0.85) was significantly higher than for CT MPI (0.78; p = 0.01), computed tomography angiography (CTA) FFR (0.78; p = 0.03), and CTA (0.70; p = 0.002).

TABLE 2 Diagnostic Performance

Modality	TP	FP	TN	FN	Sensitivity	Specificity	PPV	NPV	Accuracy
CTA	52	38	37	15	78% (65%–90%)	49% (38%–61%)	58% (48%–68%)	71% (56%–87)	63% (55%–71%)
Absolute MBF	50	29	46	17	75% (63%–86%)	61% (47%–75%)	63% (51%–76%)	73% (62%–84%)	68% (59%–76%)
CT MPI (index MBF)	49	24	51	18	73% (61%–86%)	68% (56%–80%)	67% (55%–80%)	74% (63%–85%)	70% (62%–79%)
CTA FFR	55	30	45	12	82% (72%–92%)	60% (48%–72%)	65% (55%–75%)	79% (68%–90%)	70% (63%–80%)
CTA and CTA FFR	43	18	57	24	64% (51%–77%)	76% (66%–86%)	71% (59%–82%)	70% (59%–82%)	70% (62%–79%)
CTA and CT MPI	51	17	58	16	76% (65%–87%)	77% (67%–88%)	75% (64%–86%)	78% (68%–89%)	77% (70%–84%)
CT MPI and CTA FFR	49	12	63	18	73% (61%–86%)	84% (75%–93%)	80% (70%–91%)	78% (68%–88%)	79% (71%–87%)

Diagnostic performance with invasive FFR and a threshold of ≤0.80 as reference. Dynamic CT MPI, absolute MBF using a threshold of 91 ml/100 ml/min. CTA MPI (index MBF) using a threshold of 0.71. CTA FFR using a threshold of 0.80. A predicted probability below ≥0.50 was used as a threshold for all the combined (CTA and CTA FFR, CTA and CT MPI, and CT MPI and CTA FFR) analyses.

CT = computed tomography; CTA = computed tomography angiography; FFR = fractional flow reserve; FN = false negative; FP = false positive; MBF = myocardial blood flow; MPI = myocardial perfusion imaging; NPV = negative predictive value; PPV = positive predictive value; TN = true negative; TP = true positive.

FIGURE 4 Distribution of CT-MPI, CTA-FFR, and CT-MPI Combined With CTA-FFR Is Shown, Displaying the Predicted Probabilities

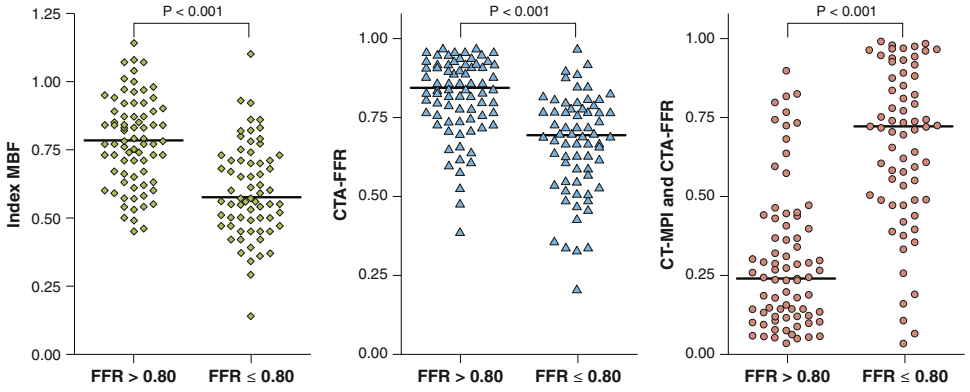

The median is displayed as a **horizontal line**. Abbreviations as in Figures 2 and 3.

CTA FFR was calculated using the Pearson correlation coefficient. The optimal threshold was calculated using the Youden index. The 95% confidence intervals were corrected for within-patient clustering of data using generalized estimating equations (20). Most statistical analyses were conducted using SPSS version 21 (IBM, Armonk, New York), while MedCalc version 13.0 (MedCalc Software, Ostend,

FIGURE 5 Diagnostic Classification by CT-MPI and CTA-FFR

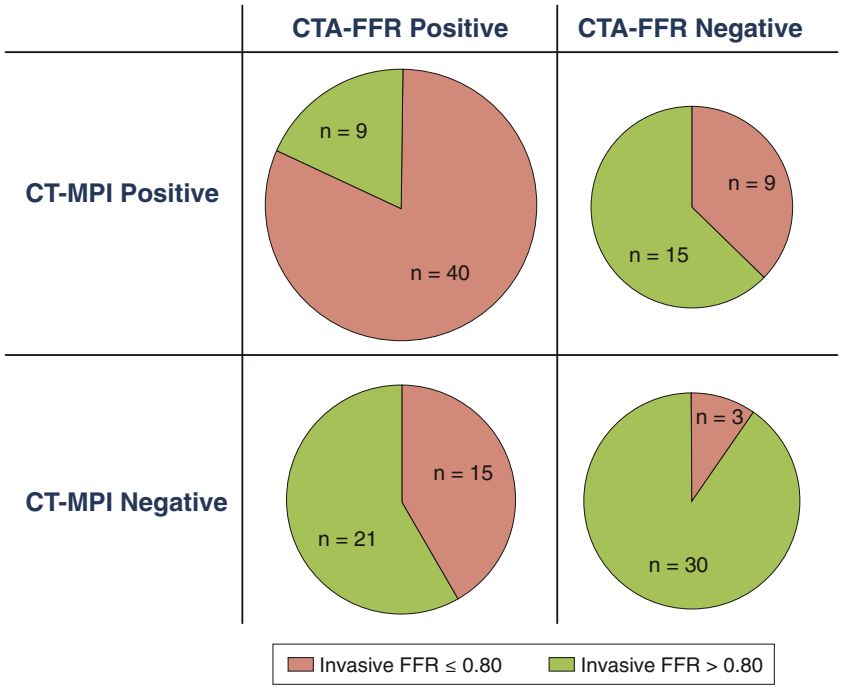

The sizes of the charts are scaled to the number of vessels and territories. Of the 49 territories and vessels classified as positive for ischemia by CTA FFR and CT MPI, 40 (82%) were confirmed by invasive FFR. Of the 33 territories and vessels for which both CTA FFR and CT MPI indicated nonfunctional stenoses, 30 (91%) were confirmed as not functionally obstructed on invasive FFR. Abbreviations as in Figures 2 and 3.

FIGURE 6 Sensitivity and Specificity With Invasive FFR as the Reference Plotted Against CTA FFR Thresholds

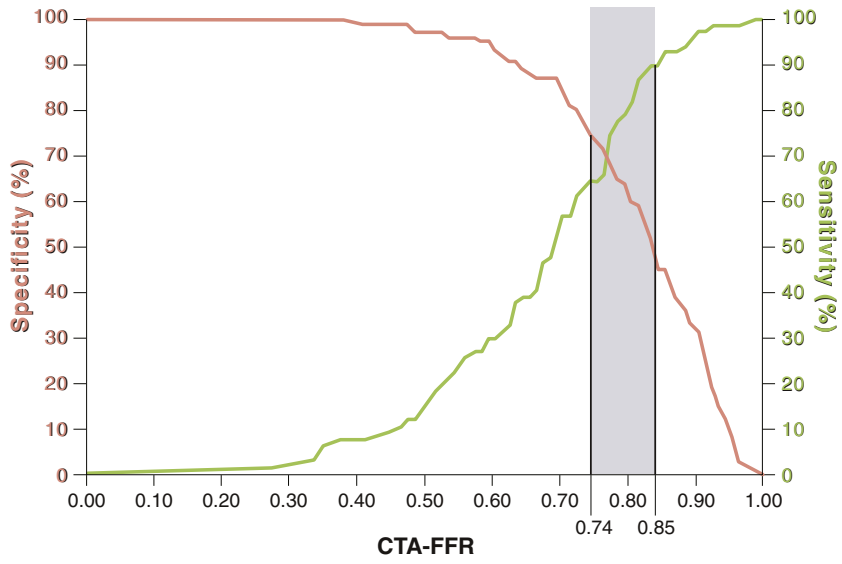

An intermediate zone was defined between sensitivity of 90% and specificity of 75%, corresponding to CTA FFR values between 0.74 and 0.85. Abbreviations as in Figures 2 and 3.

Belgium) was used to compare the areas under the curve (AUCs) using the method of DeLong et al. (21).

RESULTS

The study population consisted of 74 patients, in whom 142 vessels were investigated by invasive FFR (Figure 2, Table 1). The mean radiation dose was 3.7 ± 3.2 mSv for CTA and 9.3 ± 1.8 mSv for dynamic CT MPI. The median invasive FFR was 0.83 (IQR: 0.73 to 0.91), and 67 vessels (47%) were considered hemodynamically significant by an invasive FFR ≤0.80.

CTA. Two vessels were classified as normal, 19 as minimal, 31 as mild, 72 as moderate, 16 as severe, and 2 as occluded. The AUC for CTA was 0.70 (Figure 3). The sensitivity and specificity of CTA were 78% (95% confidence interval: 65% to 90%) and 49% (95% confidence interval: 38% to 61%) (Table 2).

DYNAMIC CT MPI. The mean absolute MBF values were 108 ml/100 ml/min for the normal (invasive FFR >0.80) territories and 79 ml/100 ml/min for the ischemic (FFR ≤0.80) territories ($p = 0.001$). The optimal threshold for absolute MBF was 91 ml/100 ml/min. Diagnostic accuracy of absolute MBF was 68% (95% confidence interval: 59% to 76%) (Table 2). The AUC was 0.75.

The mean index MBF was 0.78 ± 0.16 for normal territories and 0.60 ± 0.17 for ischemic territories ($p < 0.001$) (Figure 4). The Pearson correlation coefficient with invasive FFR was 0.48. The AUC was 0.78 (Figure 3). On the basis of the optimal threshold of 0.71 as computed with the Youden index, dynamic CT MPI correctly classified 100 of 142 territories, resulting in diagnostic accuracy of 70% (Table 2).

CTA FFR. The median CTA FFR was 0.77 (IQR: 0.66 to 0.86) for all 142 vessels and 0.84 (IQR: 0.74 to 0.92) for normal and 0.69 (IQR: 0.55 to 0.78) for ischemic territories ($p < 0.001$). Correlation with invasive FFR was 0.61. The AUC for CTA FFR was 0.78. The optimal threshold computed with the Youden index was 0.81, but in this analysis the standard threshold of 0.80 was used (Figure 3). The diagnostic accuracy of CTA FFR was 70% (Table 2). CTA FFR also correctly classified 100 of 142 vessels.

INTEGRATION OF CTA, CTA FFR, AND CT MPI. The combination of CTA and CT MPI resulted in an increased AUC of 0.83, significantly larger than either CTA or CT MPI alone ($p < 0.0001$ and $p = 0.02$, respectively).

When combining CTA and CTA FFR, the AUC increased to 0.80, significantly larger than CTA alone ($p = 0.001$), but the difference with CTA FFR (0.78, $p = 0.31$) was not significant. The combination of CT MPI and CTA FFR resulted in diagnostic accuracy of 79% (**Table 2**) and significantly increased the AUC (0.85) compared with CT MPI and CTA FFR ($p = 0.01$ and $p = 0.03$, respectively) (**Figure 3**).

Correct and concordant classification by both CT MPI and CTA FFR was accomplished in 70 of 142 vessels or territories (49%) (**Figure 5**). Stepwise diagnostic work-up was simulated to identify the patients with the largest benefit from an additional CT MPI examination following CTA FFR evaluation. An upper threshold of CTA FFR of 0.85 resulted in sensitivity of 90%, and a lower threshold of 0.74 resulted in acceptable specificity of 75% (**Figure 6**). In 44 vessels (31%), the CTA FFR value was between 0.74 and 0.85. The accuracy of CTA FFR for these 44 vessels was 55% (24 of 44) and could be improved to 77% (34 of 44) if these vessels or territories were evaluated with CT MPI instead of CTA FFR. From the total 142 vessels, this stepwise approach resulted in 110 correctly classified vessels and theoretically avoided CT MPI examinations in 34 patients (46%) and 98 (69%) of the territories.

DISCUSSION

The main findings of this study are as follows: 1) both on-site CTA FFR and dynamic CT MPI perform well in the detection of functional CAD; 2) the combination of CTA and CT MPI improves diagnostic performance, over either alone; 3) for CTA and CTA FFR, this increase was small and not significant; and 4) CTA FFR and dynamic CT MPI provide complementary information, and integrated interpretation (as a single variable) improves diagnostic performance significantly. Alternatively, both techniques can also be used in sequence, whereby selective use of CT MPI improves hemodynamic classification for intermediate CTA FFR results (0.74 to 0.85).

Dynamic CT MPI, as opposed to the previously introduced static CT MPI, acquires a series of images during the transit of contrast medium through the myocardium, which allows quantification of MBF in a way resembling quantitative MBF acquired by positron emission tomographic perfusion imaging (11,12). On the basis of the known variation in (measured) global MBF during hyperemia between scans, we applied a normalized MBF index instead of an absolute MBF threshold to classify the presence of myocardial ischemia (12,14,15). However, indexing in a way sacrifices the absolute potential of dynamic CT MPI, potentially leading to false-negative results in the presence of 3-vessel disease. A recent study by Stuijfzand et al. (22) showed that in oxgen-15-labeled water positron emission tomography perfusion, relative flow reserve did not perform significantly better than quantitative MBF assessment. The average radiation dose of a dynamic CT MPI study was 9.3 mSv, which is relatively high. However, with newer generation CT scanners, acquisition of dynamic CT MPI at lower tube voltage levels has become available, further reducing the radiation dose.

The diagnostic performance of CTA FFR alone in this study was slightly lower than in previous single-center on-site CTA FFR studies (23–25). Nakazato et al. (26) investigated the diagnostic performance of CT FFR application in a substudy of vessels with intermediate stenosis severity in the DeFACTO (Determination of Fractional Flow Reserve by Anatomic Computed Tomographic Angiography) study. The diagnostic accuracy of 69% and AUC of 0.79 were similar to the results found in our study of 70% and 0.78. However, compared with the AUC of 0.93 seen in the NXT (Analysis of Coronary Blood Flow Using CT Angiography: Next Steps) trial, diagnostic performance in this study was lower (27). The application used in the DeFACTO and NXT trials is a full-order application from HeartFlow (HeartFlow, Inc., Redwood City, California). Apart from differences in the CT FFR methodology, differences in the prevalence of hemodynamically significant disease (47% in this study vs. 21% in NXT) may have contributed to the difference in diagnostic performance (27).

In this study, CT MPI and CTA FFR performed similarly well. FFR is a derivative of coronary blood flow based on the measurement of pressure. Although there is good correlation between FFR and coronary flow, they are not entirely similar (28). In our study, the combination of both techniques significantly improved diagnostic performance in comparison with invasive FFR, supporting the notion that each technique provides incremental value. In a recent study by Yang et al. (29), the combinations of static CT MPI with CTA and CT FFR with CTA improved diagnostic performance compared with CTA alone, but those investigators used static CT MPI, as opposed to the dynamic method used in this study.

For various reasons, it is unlikely that in clinical practice both techniques will be routinely applied in each patient. Because CTA FFR requires no additional testing, we simulated a diagnostic work-up in which CTA FFR would be performed first and CT MPI only in case of an intermediate CTA FFR result.

Interpreted as a binary test, it is expected that most misclassifications occur around the threshold. Using the sensitivity-specificity plot, CTA FFR values (0.85) above which sensitivity was ≥90% and values (0.74) below which specificity was ≥75% were considered conclusive. Within the intermediate range, our results indicate that CT MPI improves interpretation of the hemodynamic significance of CAD.

STUDY LIMITATIONS. By the design of the study, and the invasive comparator, we investigated a moderate number of patients with a high disease burden. Whether the investigated techniques perform similarly in standard populations with a lower disease prevalence is currently unknown. The consecutive inclusion of patients was complicated by logistic factors such as the availability of researchers and competitive studies. Although nonconsecutive enrollment was based mainly on logistic factors, some degree of selection bias cannot be excluded.

CTA FFR and CT MPI are fundamentally different techniques for which no perfect (single) reference is available. Because invasive FFR is currently regarded as the clinical reference to assess the functional significance of CAD, we selected this technique as the most optimal comparator. Derived thresholds for both dynamic CT MPI and the combination of CTA FFR and CT MPI are based on this cohort and ideally would be validated in an external cohort.

The on-site CTA FFR used in this study was based on prototype software and is currently being used only in research settings. It is uncertain whether our results can be extrapolated to other CTA FFR or myocardial perfusion techniques.

The average radiation dose of a dynamic CT MPI study was 9.3 mSv, which is relatively high. However, with newer generation CT scanners, acquisition of dynamic CT MPI at lower tube voltage levels has become available. Preliminary observations at our institution suggest that this would further reduce radiation dose.

CONCLUSIONS

On-site CTA FFR and dynamic CT MPI are promising approaches to the functional interpretation of CAD detected on cardiac CT imaging, each demonstrating good diagnostic accuracy in comparison with invasive FFR. Integrated interpretation of both modalities further improves diagnostic accuracy. Stepwise work-up in which CT MPI is reserved for patients with intermediate CTA FFR results (0.74 to 0.85) would also improve diagnostic accuracy and could avoid MPI examinations in a substantial proportion of patients.

ADDRESS FOR CORRESPONDENCE: Dr. Adriaan Coenen, Erasmus Medical Center, Room ca-207, 's-Gravendijkwal 230, 3015 CE Rotterdam, the Netherlands. E-mail: a.coenen@erasmusmc.nl.

PERSPECTIVES

COMPETENCY IN MEDICAL KNOWLEDGE: In the work-up of patients with stable chest pain, an integrated approach combining MPI and CT FFR improves diagnostic accuracy. Diagnostic work-up in which an intermediate CT FFR result is followed by a myocardial perfusion scan could identify patients most benefiting from an additional myocardial perfusion scan, while the remaining patients would avoid additional examinations.

TRANSLATIONAL OUTLOOK: In this study, CT FFR and CT MPI were integrated. The algorithm used in this study for the integration of CT FFR and dynamic MPI can be used in future diagnostic studies. Clinical outcomes studies will be needed to investigate the additional patient benefit and cost-effectiveness of an integrated approach in the detection and treatment of CAD.

REFERENCES

1. Miller JM, Rochitte CE, Dewey M, et al. Diagnostic performance of coronary angiography by 64-row CT. N Engl J Med 2008;359:2324–36.

2. Meijboom WB, Meijs MF, Schuijf JD, et al. Diagnostic accuracy of 64-slice computed tomography coronary angiography: a prospective, multicenter, multivendor study. J Am Coll Cardiol 2008;52:2135–44.

3. Pijls NH, De Bruyne B, Peels K, et al. Measurement of fractional flow reserve to assess the functional severity of coronary-artery stenoses. N Engl J Med 1996;334:1703–8.

4. De Bruyne B, Pijls NH, Kalesan B, et al. Fractional flow reserve-guided PCI versus medical therapy in stable coronary disease. N Engl J Med 2012;367:991–1001.

5. Fihn SD, Blankenship JC, Alexander KP, et al. 2014 ACC/AHA/AATS/PCNA/SCAI/STS focused update of the guideline for the diagnosis and management of patients with stable ischemic heart disease: a report of the American College of Cardiology/American Heart Association Task Force on Practice Guidelines, and the American Association for Thoracic Surgery, Preventive Cardiovascular Nurses Association, Society for Cardiovascular Angiography and Interventions, and Society of Thoracic Surgeons. J Am Coll Cardiol 2014;64:1929–49.

6. Meijboom WB, Van Mieghem CA, van Pelt N, et al. Comprehensive assessment of coronary artery stenoses: computed tomography coronary angiography versus conventional coronary

angiography and correlation with fractional flow reserve in patients with stable angina. J Am Coll Cardiol 2008;52:636–43.

7. Ko BS, Wong DT, Cameron JD, et al. 320-Row CT coronary angiography predicts freedom from revascularisation and acts as a gatekeeper to defer invasive angiography in stable coronary artery disease: a fractional flow reserve-correlated study. Eur Radiol 2014;24:738–47.

8. Rossi A, Papadopoulou SL, Pugliese F, et al. Quantitative computed tomographic coronary angiography: does it predict functionally significant coronary stenoses? Circ Cardiovasc Imaging 2014;7:43–51.

9. Rossi A, Dharampal A, Wragg A, et al. Diagnostic performance of hyperaemic myocardial blood flow index obtained by dynamic computed tomography: does it predict functionally significant coronary lesions? Eur Heart J Cardiovasc Imaging 2014;15:85–94.

10. Raff GL, Abidov A, Achenbach S, et al. SCCT guidelines for the interpretation and reporting of coronary computed tomographic angiography. J Cardiovasc Comput Tomogr 2009;3:122–36.

11. Bamberg F, Klotz E, Flohr T, et al. Dynamic myocardial stress perfusion imaging using fast dual-source CT with alternating table positions: initial experience. Eur Radiol 2010;20:1168–73.

12. Rossi A, Merkus D, Klotz E, Mollet N, de Feyter PJ, Krestin GP. Stress myocardial perfusion: imaging with multidetector CT. Radiology 2014; 270:25–46.

13. Mahnken AH, Bruners P, Katoh M, Wildberger JE, Gunther RW, Buecker A. Dynamic multi-section CT imaging in acute myocardial infarction: preliminary animal experience. Eur Radiol 2006;16:746–52.

14. Kono AK, Coenen A, Lubbers M, et al. Relative myocardial blood flow by dynamic computed tomographic perfusion imaging predicts hemodynamic significance of coronary stenosis better than absolute blood flow. Invest Radiol 2014;49:801–7.

15. Ishida M, Kitagawa K, Ichihara T, et al. Underestimation of myocardial blood flow by dynamic perfusion CT: explanations by two-compartment model analysis and limited temporal sampling of dynamic CT. J Cardiovasc Comput Tomogr 2016; 10:207–14.

16. Ebersberger U, Marcus RP, Schoepf UJ, et al. Dynamic CT myocardial perfusion imaging: performance of 3D semi-automated evaluation software. Eur Radiol 2014;24:191–9.

17. Choy JS, Kassab GS. Scaling of myocardial mass to flow and morphometry of coronary arteries. J Appl Physiol 2008;104:1281–6.

18. Wilson RF, Wyche K, Christensen BV, Zimmer S, Laxson DD. Effects of adenosine on human coronary arterial circulation. Circulation 1990;82:1595–606.

19. Coenen A, Lubbers MM, Kurata A, et al. Coronary CT angiography derived fractional flow reserve: methodology and evaluation of a point of care algorithm. J Cardiovasc Comput Tomogr 2016;10:105–13.

20. Genders TS, Spronk S, Stijnen T, Steyerberg EW, Lesaffre E, Hunink MG. Methods for calculating sensitivity and specificity of clustered data: a tutorial. Radiology 2012;265:910–6.

21. DeLong ER, DeLong DM, Clarke-Pearson DL. Comparing the areas under two or more correlated receiver operating characteristic curves: a nonparametric approach. Biometrics 1988;44: 837–45.

22. Stuijfzand WJ, Uusitalo V, Kero T, et al. Relative flow reserve derived from quantitative perfusion imaging may not outperform stress myocardial blood flow for identification of hemodynamically significant coronary artery disease. Circ Cardiovasc Imaging 2015;8: e002400.

23. Kruk M, Wardziak L, Demkow M, et al. Workstation-based calculation of CTA-based FFR for intermediate stenosis. J Am Coll Cardiol Img 2016;9:690–9.

24. Baumann S, Wang R, Schoepf UJ, et al. Coronary CT angiography-derived fractional flow reserve correlated with invasive fractional flow reserve measurements—initial experience with a novel physician-driven algorithm. Eur Radiol 2015; 25:1201–7.

25. De Geer J, Sandstedt M, Bjorkholm A, et al. Software-based on-site estimation of fractional flow reserve using standard coronary CT angiography data. Acta Radiol 2016;57: 1186–92.

26. Nakazato R, Park HB, Berman DS, et al. Noninvasive fractional flow reserve derived from computed tomography angiography for coronary lesions of intermediate stenosis severity: results from the DeFACTO study. Circ Cardiovasc Imaging 2013;6:881–9.

27. Norgaard BL, Leipsic J, Gaur S, et al. Diagnostic performance of noninvasive fractional flow reserve derived from coronary computed tomography angiography in suspected coronary artery disease: the NXT trial (Analysis of Coronary Blood Flow Using CT Angiography: Next Steps). J Am Coll Cardiol 2014;63:1145–55.

28. Johnson NP, Kirkeeide RL, Gould KL. Is discordance of coronary flow reserve and fractional flow reserve due to methodology or clinically relevant coronary pathophysiology? J Am Coll Cardiol Img 2012;5:193–202.

29. Yang DH, Kim YH, Roh JH, et al. Diagnostic performance of on-site CT-derived fractional flow reserve versus CT perfusion. Eur Heart J Cardiovasc Imaging 2017;18: 432–40.

KEY WORDS coronary artery disease, CT angiography, CTA FFR, CT myocardial perfusion

APPENDIX For combined analysis of the performance of CTA imaging, CT MPI, and CTA FFR, please see the online version of this article.

Go to http://www.acc.org/jacc-journals-cme to take the CME quiz for this article.